

INTEGRATED GEOPHYSICAL METHODOLOGY IN A HYDROGEOLOGICAL STUDY IN THE NORTHERN COASTAL PLAIN OF RIO DE JANEIRO STATE – BRAZIL

*METODOLOGIA GEOFÍSICA INTEGRADA NUM ESTUDO HIDROGEOLÓGICO
NA PLANÍCIE COSTEIRA NORTE DO ESTADO DO RIO DE JANEIRO - BRASIL*

Abel Carrasquilla¹ & Sergio L. Fontes²

RESUMO Um estudo geofísico piloto foi realizado na Planície Litoral Norte do Estado do Rio de Janeiro (Brasil), próximo da cidade de Rio das Ostras, 200 km ao NE da cidade do Rio de Janeiro. Esta região é caracterizada pela escassez de água potável e pela existência de intrusão salina, causada principalmente pela presença de uma geologia complexa do Quaternário e por uma exploração excessiva do aquífero. A pesquisa foi realizada através do emprego de métodos geofísicos magnético e eletromagnéticos (domínios do tempo - TEM e frequência - FEM), a fim de avaliar a eficácia destes métodos nessas condições geológicas, como também, formular uma pesquisa hidrogeológica mais abrangente da região no futuro. A interpretação unidimensional (1D) dos dados dos perfis FEM e das sondagens TEM foi capaz de revelar as diferentes formações geológicas, localizando o aquífero e revelando o contato água doce – água salina. Por outro lado, o método magnético mostrou a presença de uma falha geológica com direção NE-SW, a qual fica localizada no contato geológico entre areia e argila, coincidentemente com o contato da água doce - água salina. Nossos resultados indicam um futuro promissor para a utilização de métodos geofísicos eletromagnéticos na região em prospecções de pequena escala, quanto que o método magnético confirmou a sua utilidade em estudos regionais, na indicação dos locais mais adequados para localizar poços produtivos de água potável.

Palavras Chave: geofísica, métodos eletromagnéticos, método magnético, águas subterrâneas.

ABSTRACT A geophysical pilot study has been undertaken in the Northern Coastal Plain of Rio de Janeiro State (Brazil), near Rio das Ostras Town, 200 km NE from Rio de Janeiro City. This region is characterized by both scarcity of drinking water and the existence of saline intrusions, which is caused mainly by the presence of a complex Quaternary geology and excessive aquifer exploitation. The research was performed by employing magnetic and electromagnetic methods (time - TEM and frequency - FEM domains), in order to evaluate the effectiveness of these methods under these particular geological conditions, and thus to allow the formulation of a more comprehensive hydrogeological research in the region in future. FEM profiles and one-dimensional (1D) interpretation of TEM data were capable of depicting different geological formations, to locate the main aquifer and to reveal the fresh-saline water contact. On the other hand, the magnetic method showed the presence of a NE-SW direction geological fault, which is located just in the geological contact between sand and clay, coincidentally with the fresh-saline water contact. Our results evidence a promising future for using electromagnetic geophysical methods in this region in small scale surveys, as well as it confirmed that a precursory regional survey, chiefly using the magnetic method, is essential in the indication of most suitable places to locate productive fresh-water wells.

Keywords: geophysics, electromagnetic methods, magnetic method, groundwater.

¹Laboratório de Engenharia de Petróleo – UENF, Macaé – RJ (abel@lenep.uenf.br).

²Observatório Nacional – MCT, Rio de Janeiro.

INTRODUCTION

Geographically, Rio de Janeiro State can be divided in two main regions: the Highlands region and the Coastal area. Our research was developed in a sector located in the northern portion of this last region, near São João Mount and Rio das Ostras Town (Figure 1). The regional geological map of this area shows the predominance of rocks with pre - Cambrian age, with fractures in NW/SE and NE/SW preferential directions (Figure 2). These rocks are constituted by the association of gneisses - biotites, gneisses, granites, porphyroblast - gneiss and migmatites. Locally, there are valleys filled with quaternary sediments, which were deposited in flooding plains near the coast (DRM/PETROBRAS, 1997).

FIGURE 1

FIGURE 2

The Brazilian Geological Survey (CPRM) undertook magnetometric and gamma-spectrometric air surveys covering most of Rio de Janeiro State (Mourao, 1995). The results of these surveys evidenced the major geological trends and were used as an initial guide in the present study. In another study, in the adjacent area in São Vicente District, Araruama County, MELLO (1995) made a geophysical prospecting using DC - resistivity, and the interpretation of these data revealed the existence of a granite-gneiss weathering basement with apparent resistivities (ρ_a) of 2300 - 2800 Ωm , which shows localized fractures or faults saturated with water ($\rho_a \approx 900 - 1800 \Omega\text{m}$), besides fracture-saturated C weathering ($\rho_a \approx 215 \Omega\text{m}$) and impermeable B ($\rho_a \approx 620 \Omega\text{m}$) horizons. Above the basement and in the form of a lithological discordance, there is quartz - feldspatic sandy or clayey sedimentary package, which is saturated ($\rho_a \approx 27 - 35, 78 - 100, 165 - 230 \Omega\text{m}$) and has an average thickness of 35 m. Thus, we can conclude that, excluding the

bedrock, the highest values of ρ_a are associated with geological formations presenting coarse grains and greater porosity/permeability, embedded in non-saline saturated solution. In this form, there is plenty of conditions to find fresh water in the studied region, as much in the crystalline fractured rocks as the portions where exist a thick sediment package. Therefore, with the estimation of the electrical resistivity, it is also possible to detect the zones invaded by the saline water intrusion coming from the sea, which has low ρ_a values.

METHODOLOGY

In this study, we employed electromagnetic (EM) geophysical methods in time (TEM) and frequency (FEM) domains, as well as the potential magnetic method. In the FEM method, the EM survey was performed using GEONICS EM-34 conductivity meter. This equipment is a two-man portable system comprising of a couple of coils, where one is a transmitter (Tx) and another is a receiver (Rx). When Tx is energized with an alternating current at audio frequencies (100 - 5000 Hz), the time varying magnetic field arising from this effect induces very small currents in the earth, which is assumed uniform. These currents generate a secondary magnetic field (H_s), which is sensed together with the primary field (H_p) by the receiver, in the form of total field (H_T). Thus, H_s is a complicated function of the inter-coil spacing (s), the operating frequency (f) and the ground conductivity σ (MCNEILL, 1980). With measuring signals, it is possible to study different characteristics of H_T as real (R , in phase) and imaginary (I , quadrature) component amplitudes, out-of-phase between them or dip of H_T regarding H_p , using an electrical contact between transmitter and receiver loops through a wire. In dip measuring, receiver coil is dipped until achieve the minimum or maximum values, having accurate results only when anomaly has a high conductivity. Measuring R and I components, we obtain greater values of a component or another one depending on if the sub-superficial body is a good or bad conductor,

with R/I rate growing with non-homogeneity conductivity ($\sigma=1/\rho$). However, EM-34 is designed to directly measure linear conductivity under certain constraints, defined as *operation under low induction numbers* by simply measuring the ratio between H_s and H_p . Given H_s/H_p , the apparent conductivity σ_a (mS/m) indicated by the instrument is defined as:

$$\sigma_a = \frac{1}{\rho_a} = \left(\frac{4}{(\omega\mu_0 s^2)} \right) \left(\frac{H_s}{H_p} \right), \quad (1)$$

where ω is the angular frequency ($\omega = 2\pi f$), μ_0 is the permeability of free space ($1,2566 \times 10^{-6}$ m kg C⁻²) and s is the inter-coil spacing (in m). In this case, results are generally showed in contour maps or surface profiles (WARD, 1990). The EM response at low induction numbers with either horizontal or vertical transmitter/receiver dipole orientation is based on the assumption that a) all current flow is horizontal and, b) all current loops are independent of all other current loops. This allows the construction of a function, which gives the relative response to H_s at the receiver from a thin layer of a ground at any depth. On the other hand, the coils must always be coplanar, but may be used in a vertical position or lying horizontally on the ground. The vertical coil configuration (horizontal dipoles – HD, also known as horizontal loop electromagnetic - HLEM) is the most sensitive to near surface materials and the response decreases with depth. The horizontal coil configuration (vertical dipoles – VD, also known as vertical loop electromagnetic - VLEM) has better response to materials located at a depth of approximately 0,4 s. However, materials at a depth of 1,5 s also contributes significantly. Thus, the depth of exploration is mainly a function of coil separation and orientation. The EM-34 has separate coils connected by a cable, which can be 10, 20 and 40 m long. The effective depth investigation are 7,5 m (HD) and 15 m (VD) for a frequency of 6,4 KHz and separation of 10 m. For a separation of 20 m and frequency of 1,6 Hz, is obtained a depth investigation of 15 m

(HD) and 30 m (VD), as soon as, for the separation of 40 m and frequency of 0,4 Hz, the investigation depth is 30 m (HD) and 60 m (VD) (GEONICS, 1990).

In TEM method, one strong direct current is passed through a non-grounded loop or a grounded electric dipole. At time $t = 0$, this current is interrupted and another receiving loop measures H_s produced by geological heterogeneities in subsurface in absence of inductive H_p and in the form of a declining voltage. In this curve, the electric potential is measured in different times, which are related with different geological materials in subsurface. Field procedure consists in performing several EM soundings along a profile, to show resistivities changes in distance and depth (NABIGHIAN, 1989). Generally, the results can also be showed as soundings and its 1D interpretation, but, usually, they are presented in pseudo-section form. This technique has been used to delineate stratified structures of geological interest, as well as, in the prospecting of groundwater, geothermal bodies, sulfide ores, deep graphite conductors, etc. Recently, this method has been utilized as the most efficient technique to correct the static shift, which distorts the magnetotelluric soundings (MEJU *et al.*, 1993). In our survey, we used the SIROTEM MK3 equipment, which measures the decay rate of the induction vertical magnetic component in nV/A-m², and, after that, these values are transformed in ρ_a (Ω m), as is showed in the following equation (Fitterman & Stewart, 1986):

$$\rho_a = \left[\left(\frac{\mu}{4\pi} \right) \left(\frac{b^2 A^2}{5tV} \right) \right]^{2/3}, \quad (2)$$

where μ is magnetic permeability ($1,2566 \times 10^{-6}$ m kg C⁻²), b is the side of the transmitter loop (in m), A is the effective area of the receiver loop (area x number of coils), I is the electrical current in the transmitter loop (Amp), V is the transient voltage (Volts) and t , the time since the beginning of the transient (s).

Magnetic survey methods, meanwhile, have a broad range of applications, from small-scale environmental, engineering and archaeological surveys to detect buried magnetic objects, to large-scale surveys for investigating regional geological structures. In our study, the magnetic data were gathered with two SCINTREX WALKMAG proton-precession magnetometers, which measure the scalar magnitude of the total field in nanoTesla (nT). One of the magnetometers was fixed in a base station to measure the diurnal variation in the magnetic field intensity. This kind of magnetometer gives a series of discrete measurements at intervals of a few seconds, because of the polarizing and relaxing time taken by protons (SHARMA, 1997).

In fieldwork, with these geophysical methods, we performed profiles in a N-S direction, between São João Mount and the beach, through 17 TEM soundings along 3 km of extension, beside FEM profiles were fulfilled in a small sector of the greater profile (beginning in the second station in W-E direction) with 330 m of extension and station spacing of 5 m (Figure 5). On the other hand, magnetometric profiles were made in the same form and location, but only with 1 km extension, with station spacing of 1 m. Another two parallel magnetic profiles were made 250 m E and W from the first one, respectively (P1 and P2).

RESULTS

Figure 3 shows the FEM profiles with both VD and HD arrays, while Figure 6 shows the relative positions of these profiles regarding the longest one. In the qualitative interpretation of these data, we can observe a higher ρ_a (50 Ωm or more) at the initial stages of the curves, which is related with a dune sandy terrain. After 150 m, the ρ_a values decrease to about less than 10 Ωm , showing the presence of clayey terrain, probably saturated with saline water. HD profiles are more smooth, whereas VD show larger ρ_a variations in subsurface caused by heterogeneities. These values decreased with

depth (curves with Tx-Rx = 40, 20 and 10 m, and frequencies = 0.4, 1.6 e 6.4 KHz, respectively), possibility due to greater water saturation in the geological formations below the water table. On the other hand, in the end of the profiles, the VD curves show a heterogeneity that increase its size and with depth, possible caused by local sand lenses.

FIGURE 3

In the TEM data interpretation, we used the dumped least squares inversion algorithm for horizontal layers (ridge regression), using the TEMIXXL program manufactured by INTERPEX (1996). The exact positions of two of these interpreted soundings are shown in Figure 6. The first one, corresponding to the Sounding 1, has 6% of fitting error and was performed in the sector W of the profile, above sandy terrains (Figure 4). The second one is the Sounding 4, which is located at Sector E, above clayey terrains, possibly saturated with salty water (Figure 5). Thus, the interpretation of the 17 soundings shows the presence of four horizons: a) the first one is the soil, with $\rho_a \approx 12 \Omega\text{m}$ and thickness varying between 10 - 24 m; b) the second is a resistive layer, located at the Sector W of the profile (with ρ_a between 40-105 Ωm , and $h \approx 4 - 30 \text{ m}$) and a very conductive layer in the E part of the section ($\rho_a \approx 0,2 - 0,7 \Omega\text{m}$ and $h \approx 3 - 5 \text{ m}$); c) the third is a slightly resistive layer, with $\rho_a \approx 100 \Omega\text{m}$ and $h \approx 30 \text{ m}$, in Sector W, and, $\rho_a \approx 10 \Omega\text{m}$ and $h \approx 4 - 8 \text{ m}$ in Sector E; and d) the fourth, is the crystalline basement, with $\rho_a \approx 1000 - 5000 \Omega\text{m}$. The geo-electrical section derived from the TEM soundings shows higher values of ρ_a in the Sector N (sand) compared to ρ in the Sector S (clay with salty water), as well as the presence of a crystalline basement at higher depths (Figure 6). In the same figure, between the distances of 370 m and 700 m, it is also shown the relative positions of FEM measurements, which show results with similar features to TEM ones - in both data sets the ρ_a values vary

between 50 Ωm to less than 10 Ωm (compare Figures 3 and 6). The more resistive deep heterogeneity showed in the end of FEM profiles is also seen in the TEM geoelectrical section, near 700 m. In the coincident part of FEM profiles and TEM geoelectrical section, it is also evident that Sector W shows a resistive sandy material with high porosities/permeabilities, where fresh water is known to exist. The higher thickness of the aquifer in the Sector W of the profile can be associated with the presence of a fracture or a geological fault with NE/SW strike direction.

FIGURE 4

FIGURE 5

FIGURE 6

On the other hand, Figure 7 shows the magnetic map and profiles made in the survey area. We performed three profiles in the area, one in the same position of the EM (TEM and FEM) profiles (P3) and the two others (P1 and P2) in parallel lines, separated by a distance of 400 m between each other. After common magnetic data processing (diurnal correction, regional – local separation, etc.), it was made the interpretation of one of the profiles (Figure 8), which clearly exhibits the pattern of fault anomalies (minimum of 23600 and maximum of 23700 nt), joint with the relief of bedrock. The interpretations of the profiles were made using WINGLINK software (GEOSYSTEM 2000). Thus, profile P3 shows coincident patterns with those detected with FEM profiles (Figure 3) and TEM geoelectrical section (Figure 6), i.e., presence of a fault and crystalline basement relief.

FIGURE 7

FIGURE 8

CONCLUSIONS

The results of this study show the feasibility of using EM and magnetic geophysical techniques in contributing for the solution of several problems: the determination of fresh/saline water contact, the location of geological structures such as faults, the delimitation of the aquifers and the indication of the best locations to drill water wells in this sector of the North Fluminense Coastal Plains in Rio de Janeiro State, Brazil. The TEM method was useful in both showing the layered structure (sand, clay and bedrock) and in defining the resistive/conductive contacts, marked with the presence of saline water intrusions and a fault in the crystalline basement, probably refilled with sandy material. On the other hand, the FEM method has proved to be a fast recognizing technique to determine both lateral variations and fresh/saline water contacts in geological formations. Finally, with the addition of magnetic data, the obtained results depict the existence of a fault in the NE/SW direction, as it is shown in the main family of faults of Figure 2, and the bedrock topography. These results suggest that these methods together can be employed as complementary tools in more extensive hydrogeological studies, as planned in a future for a larger region covering the studied area.

REFERENCES

- DRM/PETROBRAS. 1997. **Mapa Geológico do Estado do Rio de Janeiro, escala 1:400000.**
- FITTERMAN D. V. & STEWART M. T. 1986. **Transient electromagnetic sounding for groundwater.** Geophysics vol. 51, no 4, p: 995-1005.
- GEONICS. 1990. EM-34 Users Manual, 234 pp.
- GEOSYSTEM. 2000. **Integrated Geophysical Interpretation Software for Windows 95/98/NT, WINGLINK™ version 1.44. User's Guide.** Milan, Italy, 182 pp.
- INTERPEX, *Ltd.* 1996. **TEMIXXL Software, User's Guide,** Vol. I e II.
- MCNEILL, J.D. 1980. **Electrical conductivity of soils and rocks.** Technical Note TN-5. GEONICS Ltd., Mississauga, Canada, 21 p.
- MEJU, M.A., FONTES, S.L. & OLIVEIRA, M.F.B. 1993. **Joint TEM/AMT feasibility studies in Parnaíba basin, Brazil: Geoelectrostratigraphy and Groundwater Resource evaluation in Piauí State,** Proceedings of the 3rd International Congress of the Brazilian Geophysical Society, Vol. 2, 1373-1378.
- MELLO, L.C. 1995. **Possibilidade de água subterrânea como alternativa na recuperação da citricultura no Distrito de São Vicente, Município de Araruama - RJ.** Proceedings of the 4th International Congress of the Brazilian Geophysical Society, Vol. 2, 1013-1016.
- MOURÃO, L.M.F. 1995. **Base de dados de projetos aerogeofísicos do Brasil (Aero).** Proceedings of the 4th International Congress of the Brazilian Geophysical Society, Vol. 1, 237-239.
- NABIGHIAN, M.N. 1987. **Electromagnetic methods in applied geophysics. I. Theory and Vol. II, Applications, Parts A and B.** Society of Exploration Geophysicist, Tulsa. 513 and 972 pp.
- SHARMA, P.V. 1997. **Environmental and engineering geophysics.** Cambridge University Press, 475 p.
- WARD, S.H. 1990. **Geotechnical and Environmental Geophysics. Vol. I: Review and Tutorial; Vol. II: Environmental and Groundwater; Vol. III: Geotechnical.** Society of Exploration Geophysicist, Tulsa. 389, 342 and 300 pp.

ACKNOWLEDGEMENTS

This work was sponsored by a grant from Brazilian Program for Support the Development of Science and Technology (PADCT III). We also acknowledge the Brazilian Research Council (CNPq) for providing research fellowships. We thank Prof. Miguel Mane from Rio de Janeiro State University (UERJ) for making available to us the magnetic field data of the survey area.

FIGURE CAPTIONS

Figure 1. Location of survey area.

Figura 1. Localização da área de estudo.

Figure 2. Geological map of studied area: homogeneous granites (red), metamorphic rocks derived from sedimentary rocks (blue), magmatic alkaline rocks (green), quaternary sediments (yellow), metamorphic rocks derived from igneous rocks (pink) and tertiary sediments (orange).

Figure 2. Mapa geológico da área estudada: granitos homogêneos (vermelho), rochas metamórficas derivadas de rochas sedimentárias (azul), rochas magmáticas alcalinas (verde), sedimentos cuaternários (amarelo), rochas metamórficas derivadas de rochas ígneas (rosa) e sedimentos terciários (laranja).

Figure 3. FEM profiles.

Figura 3. Perfis FEM.

Figure 4. TEM Sounding 1 in Sector N and its interpretation.

Figura 4. Sondagem TEM 1 no Setor N e sua interpretação.

Figure 5. TEM Sounding 4 in Sector S and its interpretation.

Figura 5. Sondagem TEM 4 no Setor S e sua interpretação..

Figure 6. TEM geoelectrical section.

Figura 6. Seção geolétrica TEM.

Figure 7. Magnetic map of the studied area.

Figura 7. Mapa magnético da área estudada.

Figure 8. Interpretation of the P3 magnetic profile.

Figura 8. Interpretação do perfil magnético P3.

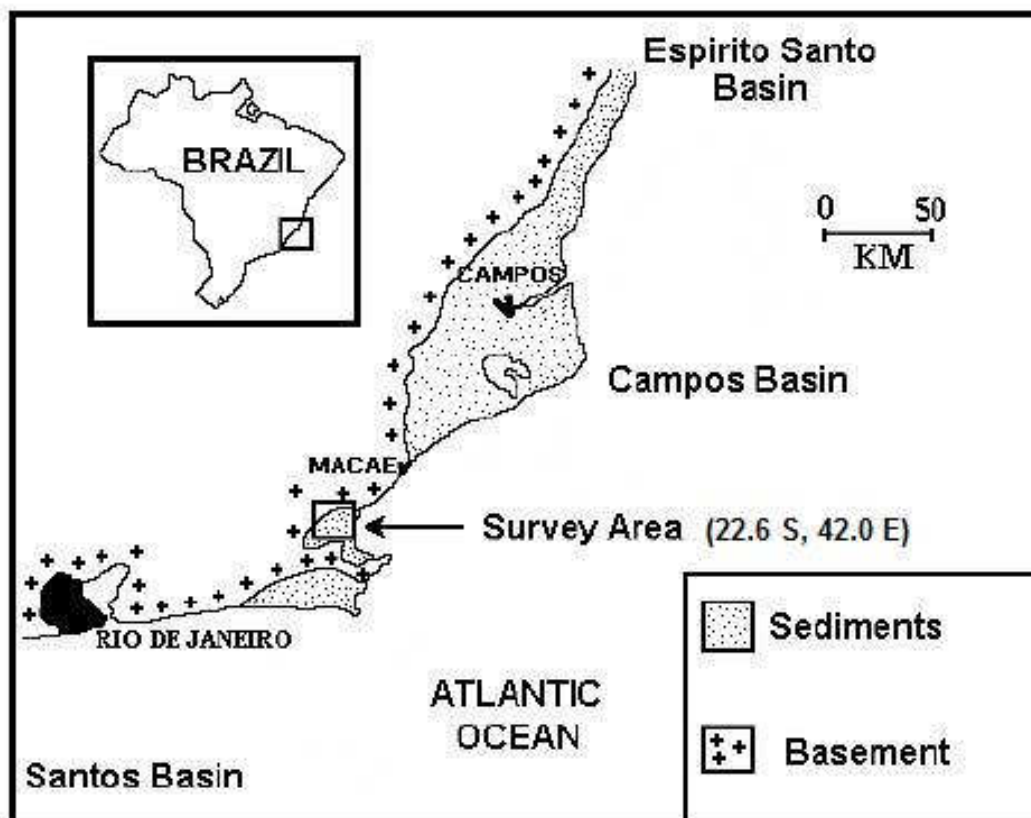


Figure 1. Location of survey area.

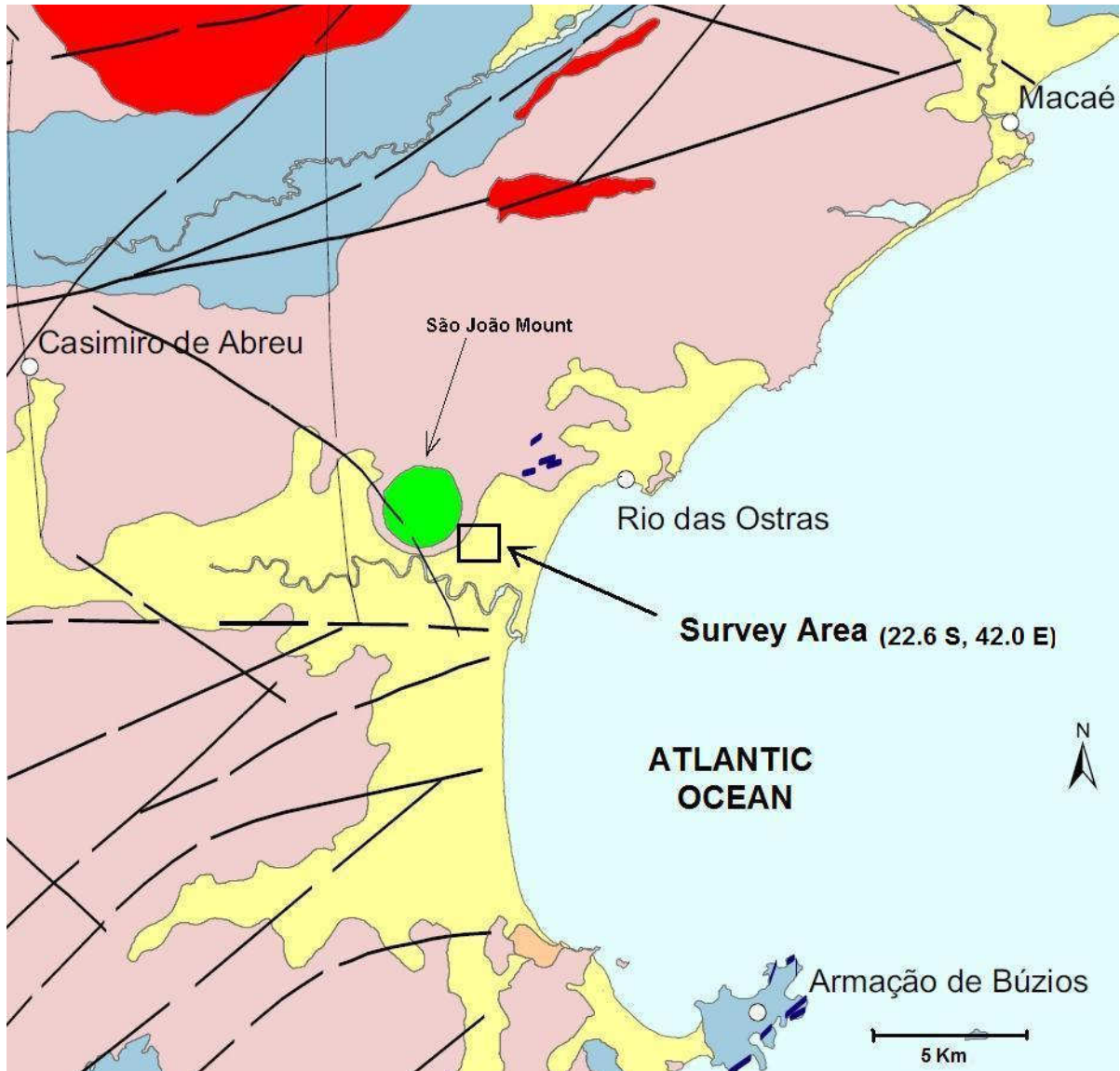


Figure 2. Geological map of studied area: homogeneous granites (red), metamorphic rocks derived from sedimentary rocks (blue), magmatic alkaline rocks (green), quaternary sediments (yellow), metamorphic rocks derived from igneous rocks (pink) and tertiary sediments (orange).

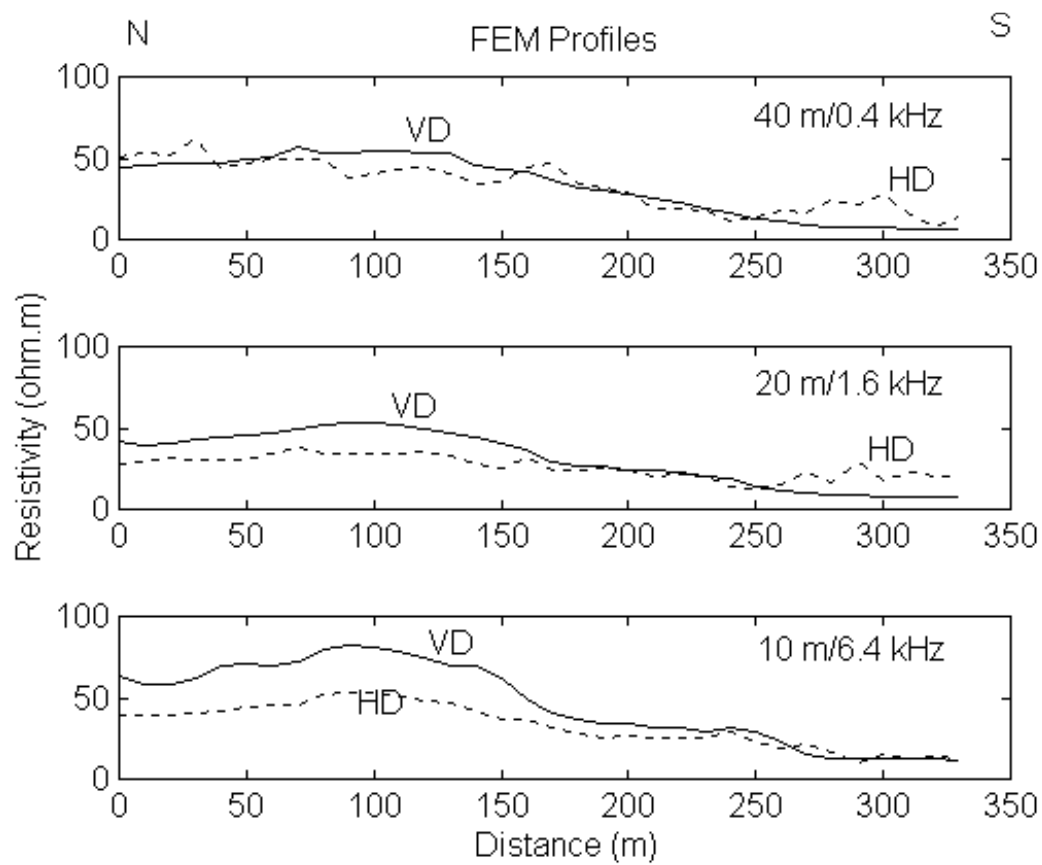
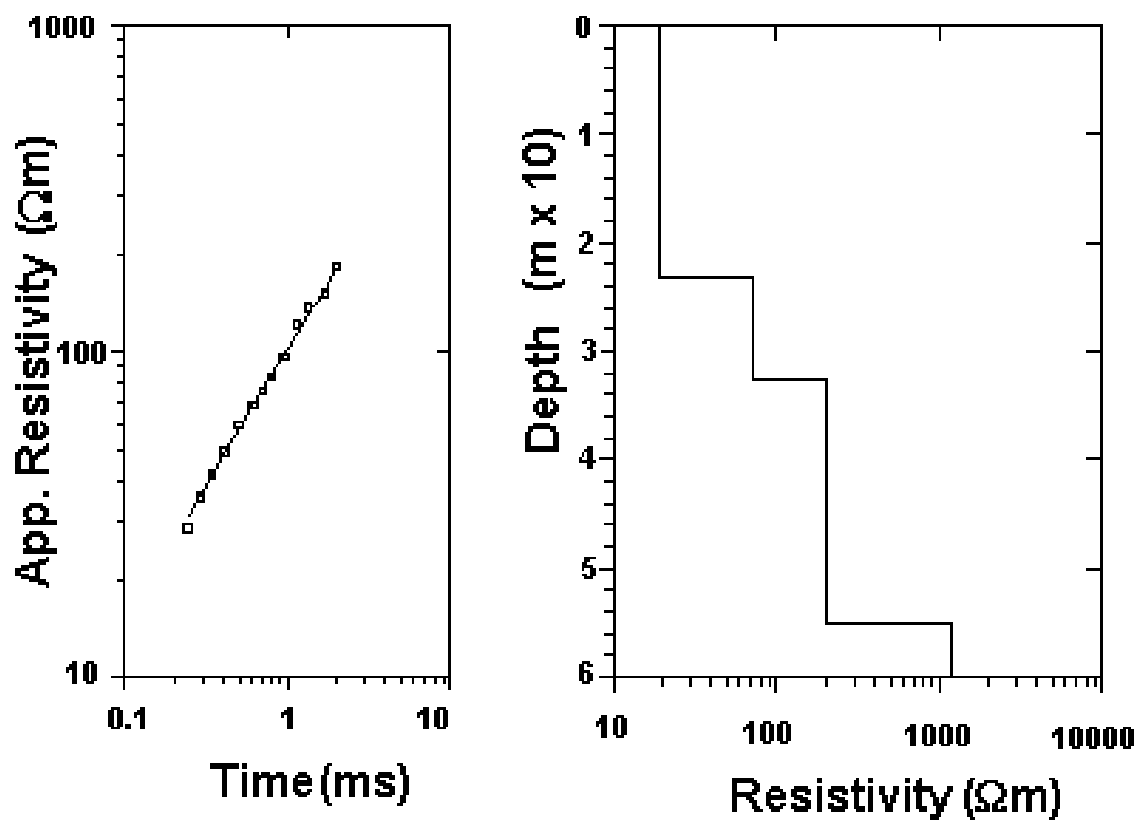


Figure 3. FEM profiles.



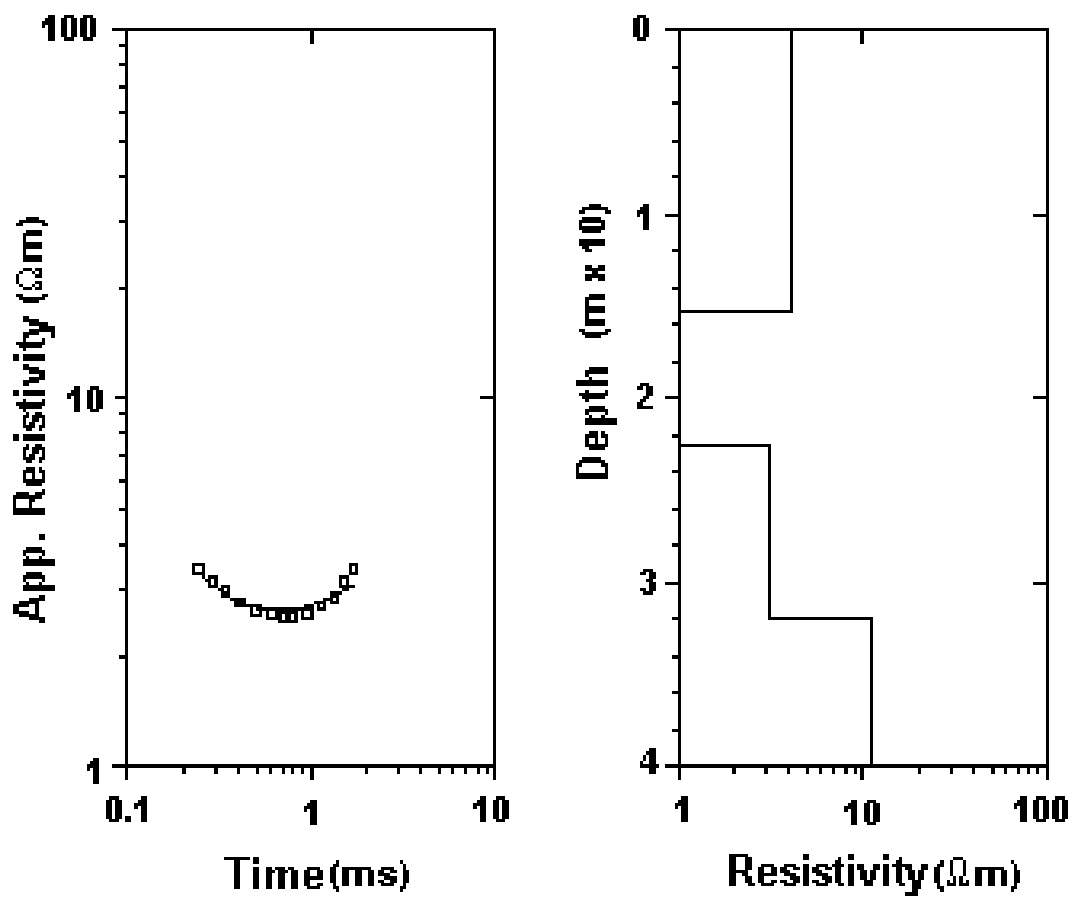


Figure 5. TEM Sounding 4 in Sector S and its interpretation.

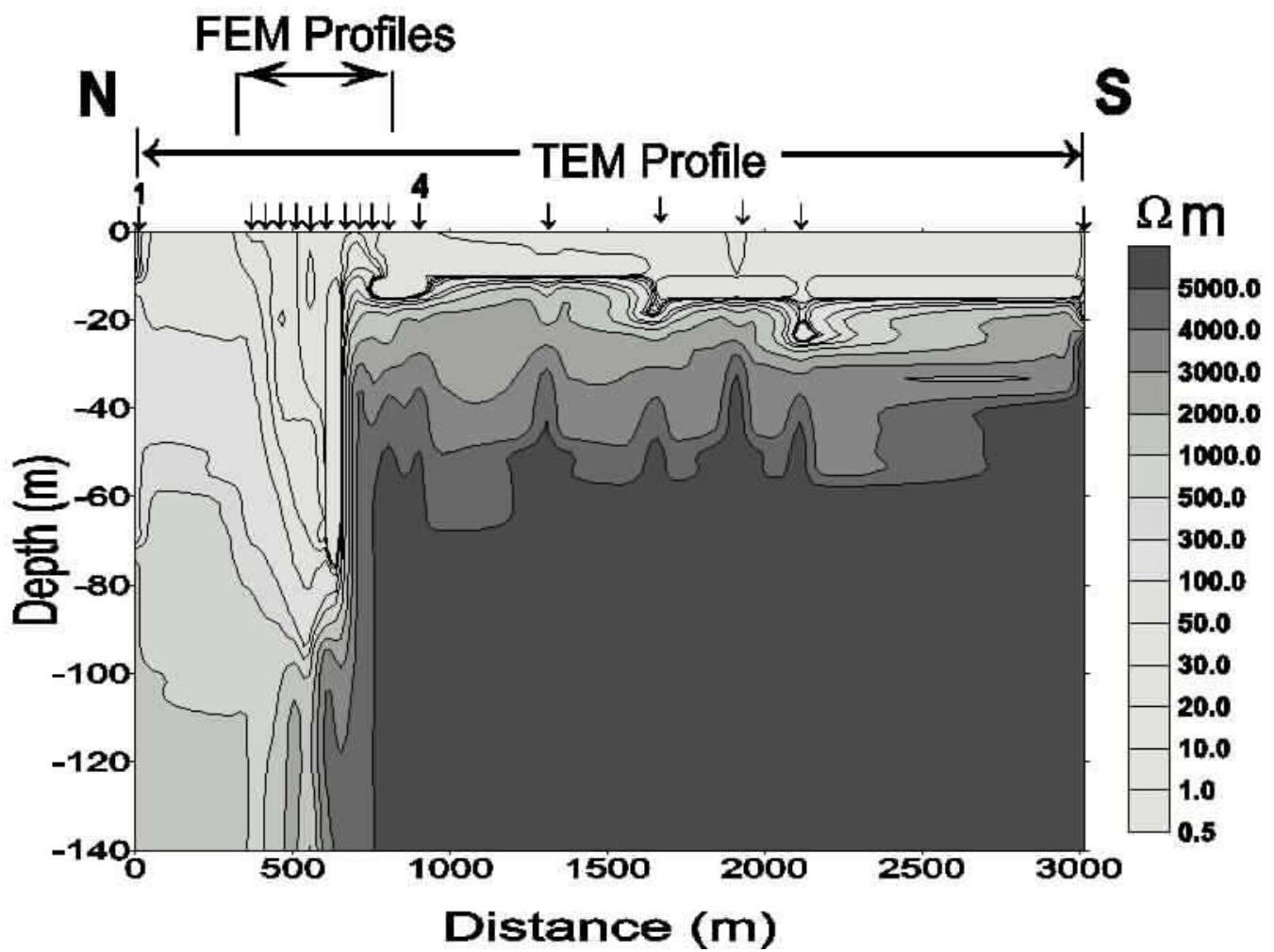


Figure 6. TEM geoelectrical section, where each arrow means the position of an electromagnetic sounding.

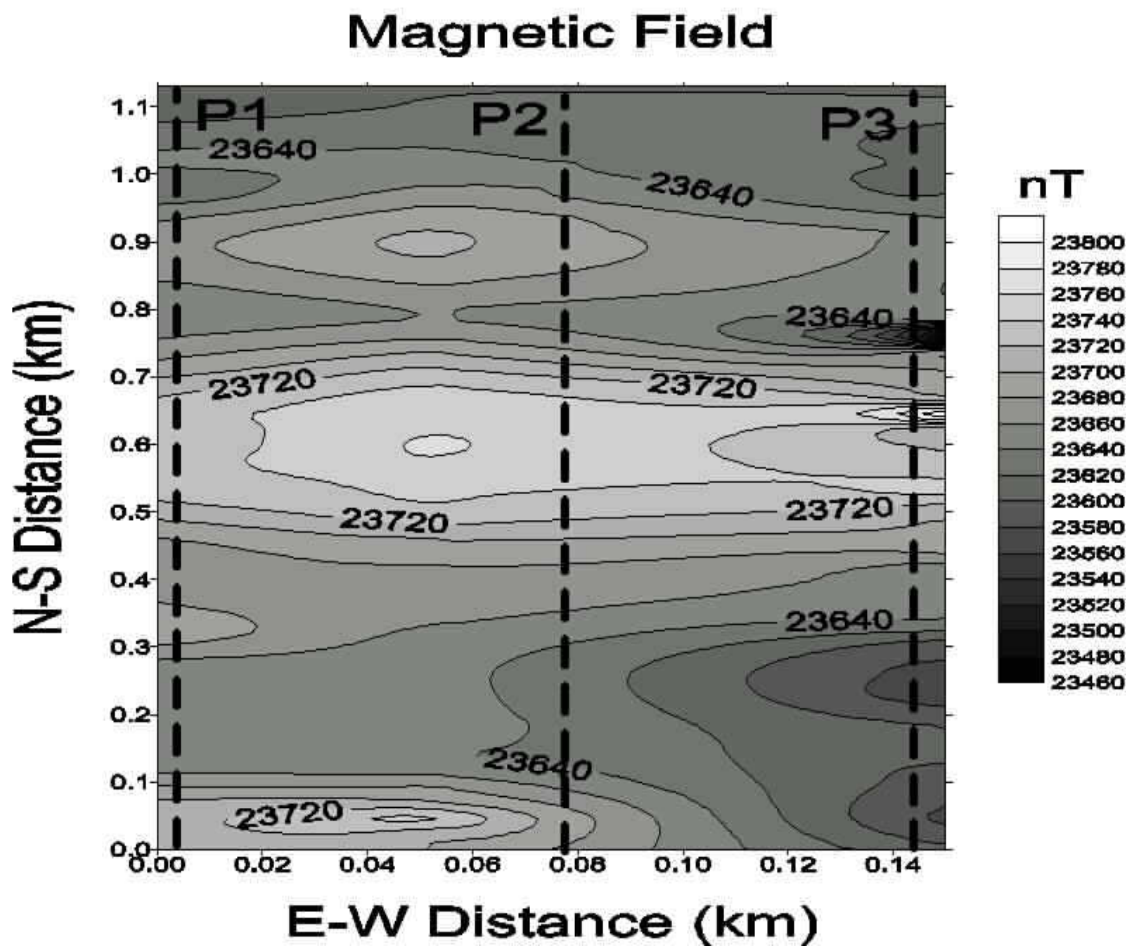


Figure 7. Magnetic map of the studied area.

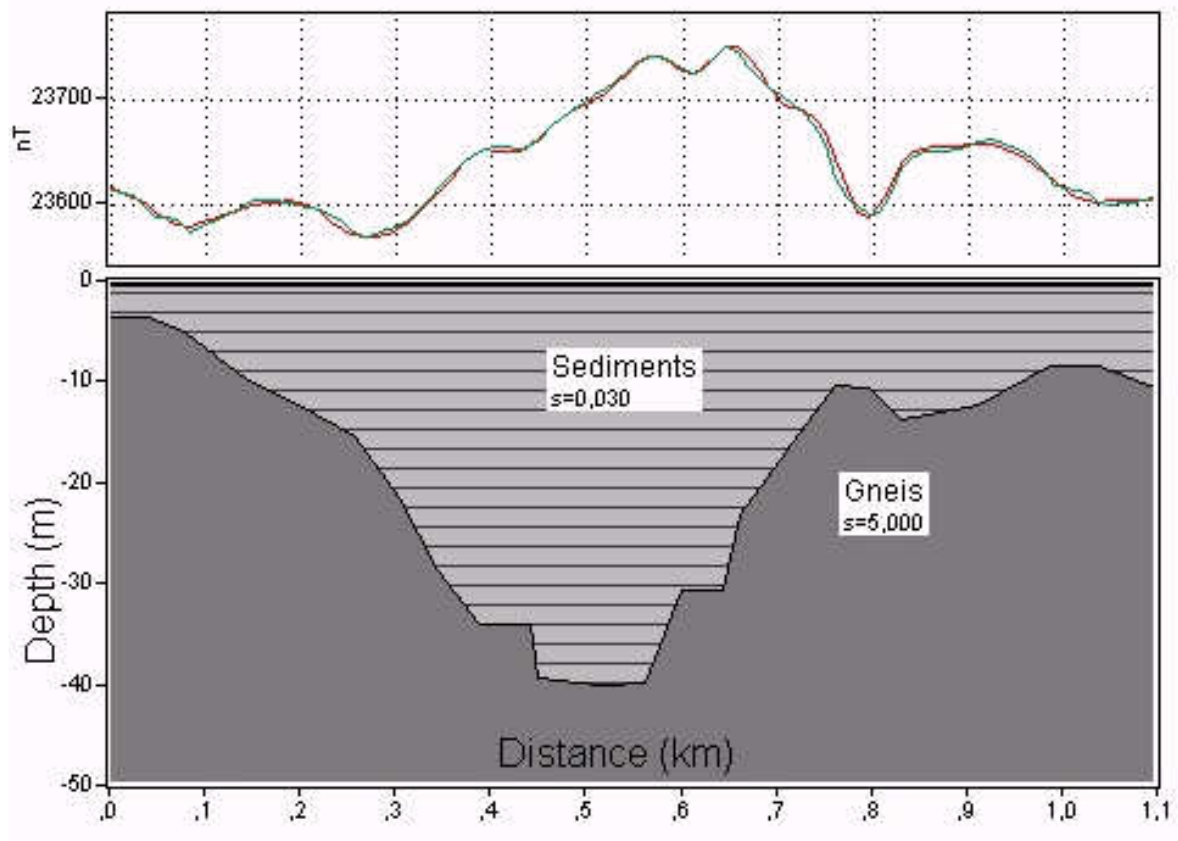


Figure 8. Interpretation of the P3 magnetic profile.